

Estimation of correlation between microphysical properties and chemical composition of aerosol over the White Sea

V.V. Pol'kin, L.P. Golobokova,¹ V.S. Kozlov, V.B. Korobov,²
A.P. Lisitsyn,³ M.V. Panchenko, M.A. Peskova,²
T.V. Khodzher,¹ and V.P. Shevchenko³

*Institute of Atmospheric Optics,
Siberian Branch of the Russian Academy of Sciences, Tomsk*
¹ *Linnological Institute,*

Siberian Branch of the Russian Academy of Sciences, Irkutsk

² *Arkhangelsk Center for Hydrometeorology and Environmental Monitoring with Regional Functions*

³ *Institute of Oceanology,
Russian Academy of Sciences, Moscow*

Received April 5, 2004

We present some results on the mass concentration of soot, chemical composition, number density, and the microstructure of the aerosol in the surface atmospheric layer obtained over various areas of the White Sea. These data have been collected during the 55th mission of the *Professor Shtokman* research vessel. We also consider the correlation between chemical elements (ions) content in the aerosol matter and disperse composition of aerosol particles.

Introduction

As known, the environment in the northern regions is very sensitive to anthropogenic impact, and the atmosphere is one of the main channels of the environmental pollution at high latitudes.^{1,2}

To study the spatiotemporal variability of the aerosol parameters over sea, as well as the correlation between the aerosol chemical composition and the disperse structure in various regions of the White Sea, the experiments involving measurements of the aerosol microstructure, number density, and chemical composition, as well as the mass concentration of soot have been carried out on August 20–31 of 2003 during the 55th mission of the *Professor Shtokman* research vessel.^{3,4}

The earlier proposed approach⁵ using the combined data on the microstructure and the chemical composition of atmospheric particles allows us to estimate the contribution of continental and marine sources to formation of the aerosol over the White Sea.

Experimental instrumentation and techniques

The disperse composition of aerosol was studied with an AZ-5 automated photoelectric counter (256 size intervals ranging from 0.4 to 10 μm of the particle diameter) and a PKGTA 0.3-002 photoelectric counter (6 size intervals from 0.3 to 1 μm). The AZ-5 sampler was placed on the port side of the vessel in the lab at the height about 4 m above the water surface.

The measurements have been carried out round-the-clock every hour (24 measurements a day). In contrast to earlier investigations,^{5,6} the AZ-5 counter included a specialized spectrum analyzer developed at the Laboratory of Aerosol Optics (Institute of Atmospheric Optics SB RAS). The analyzer was connected to a personal computer.

During the mission, an overall of 240 size spectra of aerosol particles were measured using the automated counter. The PKGTA counter was set on the upper deck at the starboard at the height of about 8 m above the water surface. The measurements were mostly conducted in daytime with the one-hour interval. About 70 size spectra were measured with the PKGTA counter over the White Sea.

For determining the chemical composition of the aerosol, we used sampling onto filters. Aerosol sampling was conducted with two devices: standard aspirator and 3-cascade impactor. The air was blown through the aspirator channel by a Model 822 blower at a rate of 20 liter/min and a 5-liter/min rate through the impactor channel. Filters were made of the Whatman (U.K.) chemically clear filtering paper. The aerosol sampler was installed on the upper deck – in the zone of minimum distorting effect of the vessel. The cascade impactor used sequentially three stages with the inlet diameters $d_1 = 7.9$ mm, $d_2 = 5.0$ mm, and $d_3 = 3.2$ mm. Particles nondeposited on an obstacle and having passed through the next impactor cascade, were collected onto filters. Using this aerosol sampling technique, chemical analysis can be performed for four size fractions of the aerosol with the particle diameter greater than 1 μm . The periodicity

of aerosol sampling onto the aspirator filters was 1–2 times a day. The sampling with the impactor was carried out at the same time sequentially for the four cascades. Depending on the aerosol and weather conditions, the sampling onto the aspirator filters took from 4 to 14 h and that onto the impactor filters took from 1.5 to 3 h per one cascade. During the mission, 9 aerosol samples were collected with the aspirator, and 36 samples were collected with the impactor.

The ion composition: H^+ , Na^+ , K^+ , Ca^{2+} , Mg^{2+} , NH_4^+ , Cl^- , NO_3^- , HCO_3^- , SO_4^{2-} was determined under laboratory conditions. The concentration of hydrogen ions (H^+) in aerosol was not determined directly, but calculated from the measurements of pH of the aqueous filter extract to close the ion balance, that is, to check the correctness of the determination.

The anion composition of the soluble fraction of aerosols after extraction from the filters by the bidistilled water was determined by the high-performance liquid chromatography (HPLC) method (Milikhrom A-02 microbore chromatograph with the error of 4–7%). The cation composition was determined by flame atomic absorption spectrometry with air-acetylene flame (AAS-30 spectrophotometer with the error of 4–6%). The insoluble part will be studied by the neutron activation method and is not discussed in this paper.

The mass concentration of soot M_s [$\mu\text{g}/\text{m}^3$] was studied with a specialized optical meter of the soot content developed at the Laboratory of Aerosol Optics, IAO SB RAS.⁷ In the operating principle, this meter is similar to the aethalometer designed by Hansen, Rosen, and Novakov.⁸ The operation of the meter is based on the continuous measurement of diffuse extinction of radiation by a layer of aerosol particles in the process of their deposition onto a filter from the air blown. The value of the measured diffuse extinction is directly proportional to the surface concentration of soot on the filter and, consequently, to its mass concentration in air.^{9,10} The absolute calibration of aethalometer was carried out by comparing the data of synchronous optical and gravimetric measurements of the soot aerosol.¹¹ The mass concentration of soot was measured automatically round-the-clock with the interval of 1 h. During the mission, an overall 239 series of the mass concentration of soot in the atmosphere over the White Sea were recorded.

Along with these techniques of aerosol sampling onto filters, we used the technique of collecting beryllium (^7Be) isotopes onto a Petryanov filter, which gives an independent estimate of the aerosol flow onto the ground. The studies by this technique are beyond the scope of this paper.

The use of the impactor, whose cascades have different efficiency of deposition of large particles greater than $1\ \mu\text{m}$, has allowed us to estimate the content of some ions in the particles of the coarse aerosol fraction.

The deposition efficiency of the impactor cascades was checked experimentally using an automated photoelectric counter of aerosol particles, which belongs to the Aerosol Station of the Laboratory of Aerosol Optics of the Institute of Atmospheric Optics SB RAS.

Figure 1 shows the concentration of particles of different size ranges normalized to $N_{0.2}$ ($r = 0.2$ – $0.25\ \mu\text{m}$) upon passage through the impactor cascades along with the cascade efficiency calculated assuming 100% of all particles to pass through in the absence of the cascades. The deposition efficiency for the first cascade (inlet diameter $d_1 = 7.9\ \text{mm}$) was about 20% for particles with $r > 0.5\ \mu\text{m}$, for the second cascade ($d_2 = 5\ \text{mm}$) it was 40% for particles with $r > 0.6\ \mu\text{m}$, and for the third cascade ($d_3 = 3.2\ \text{mm}$) it was 60% for particles with $r > 0.9\ \mu\text{m}$.

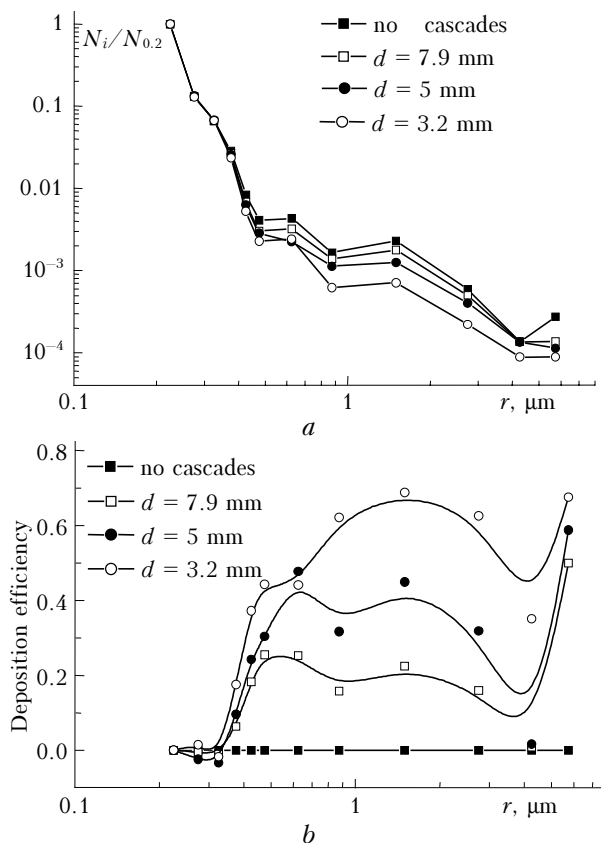


Fig. 1. Estimated efficiency of aerosol particle deposition by impactor cascades: (a) concentration ratio of particles of different size ranges N_i to those of the first range $N_{0.2}$ upon passage through the impactor cascades; (b) efficiency of every cascade.

The collection of the aerosol matter onto the impactor filters was organized as follows. Every cascade, installed in turn, collected particles with the size greater than r_i on the obstacle. Aerosol particles passed through the cascade were deposited on the filters. Consequently, each cascade cut off, with different efficiency, aerosol particles with large size.

If the chemical element under study was mostly contained in coarse particles, then its concentration was maximal on the filter without installation of the impactor cascades and minimal on the filter after the cascade with the maximal deposition of large particles ($d_3 = 3.2\ \text{mm}$). The concentrations for other cascades occupied the intermediate position. In this case, it was believed that the contributions from the impactor cascades are separated.

General characterization of the region and brief review of synoptic situation

The aerosol characteristics were studied during the 55th mission of the *Professor Shtokman* research vessel. The map of sampling along the RV route is shown in Fig. 2. Digits mark the places of aerosol sampling by the aspirator and the impactor. The synoptic situation in the period of August 20–31 was the following.

On August 20 the White Sea was affected by the south-west periphery of the cyclone, whose center lied over the southern New Land. Gentle breeze of variable direction was observed in the surface layer (the pressure increased). Northwestern and western flows prevailed in the middle atmosphere.

On August 21 an intermediate ridge was located over the White Sea. The pressure in the surface layer increased. The baric field changed in the middle troposphere. The high-altitude flows altered to southwestern ones.

On August 22–23, as the intermediate ridge left the region, the slow-moving cyclone with the center over the Gulf of Bothnia began to affect the area of the White Sea (the surface pressure decreased). The southeastern and southern wind with the mean velocity of 5 m/s prevailed in the surface layer. The decrease of the geopotential was observed on the baric topography maps. At 850 hPa the heat (up to +8°)

ridge extended to the western areas of the White Sea, and the thermal gradients increased.

On August 25 the intermediate ridge of the anticyclone centered over Norway extended to the White Sea. The mean surface wind was about 4–6 m/s.

Since August 26 active cyclones from the southwest began to move through the area of the White Sea. In this connection, the meteorological elements in the surface atmospheric layer changed sharply. The wind over the sea grew up to 8–10 m/s. The thermal and baric gradients increased at all altitudes.

On August 27 the cyclone center was located over the White Sea, and therefore the surface wind temporarily became weakened down to 2–4 m/s. The weather in the cyclone center was characterized by the presence of fogs.

On August 31 a new cyclone from the Vologda Region began to move to the territory of the White Sea.

Thus, the synoptic and meteorological situations in the area of measurements were mostly characterized as cyclonic with high cloud cover index (up to 10) with short period (August 25–26) of anticyclone (cloud cover index of 5–8). Slight force 2–3 storms and one force 4–5 storm (August 26–27) with the income of cyclone were observed. The air temperature varied from 10 to 14°C, and the water temperature was about 12°C.

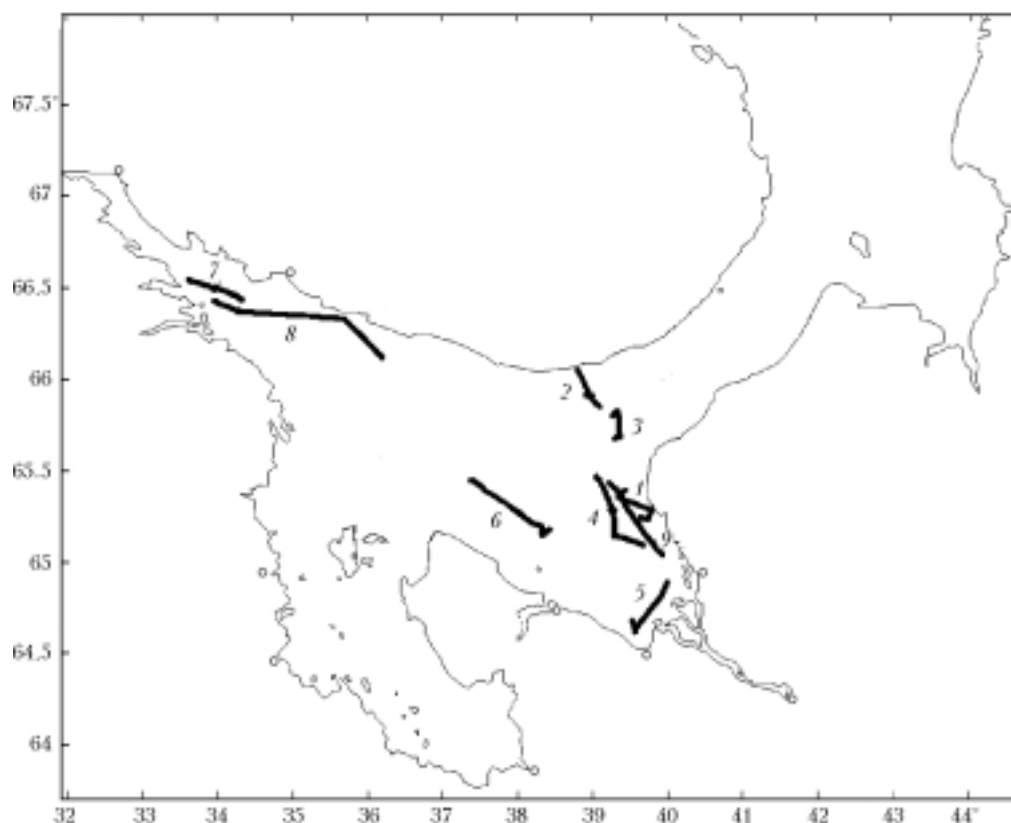


Fig. 2. Map of the 55th mission of the *Professor Shtokman* RV with numbered places of aerosol sampling by aspirator and impactor: August 21 (1); August 22 (since 7:30 to 15:20 Moscow time) (2); August 22 (since 17:10 to 21:30 Moscow time) (3); August 23 (4); August 24 (5); August 25 (6); August 27 (7); August 28 (8); August 30 (9).

Analysis of the experimental data

The general time behavior of the mass concentration of soot, $\mu\text{g}/\text{m}^3$ and the number density of particles larger than $0.4 \mu\text{m}$ measured with the AZ-5 and PKGTA counters, in cm^{-3} , is shown in Fig. 3. The periods of aerosol sampling onto the aspirator and impactor filters and onto the Petryanov filtering cloth are indicated. Figure 3 shows also the dynamics of the following surface meteorological parameters: wind velocity, m/s , pressure, mm Hg , and air temperature, $^{\circ}\text{C}$, along with the data on the sea roughness.

It is worth noting that the total number density of aerosol particles and the soot concentration was enhanced in the areas near industrial and coastal regions (see Figs. 2 and 3).

In analysis of the data on the mass concentration of soot and microstructure parameters, we took into account the effect of the disturbing factor, such as local anthropogenic sources (smoke, diesel engine exhausts, air funnel emissions). These factors show themselves in the sharp increase of the measured parameters. This is illustrated by Fig. 3 (August 23 and 24). The distorted data were rejected from the further analysis.

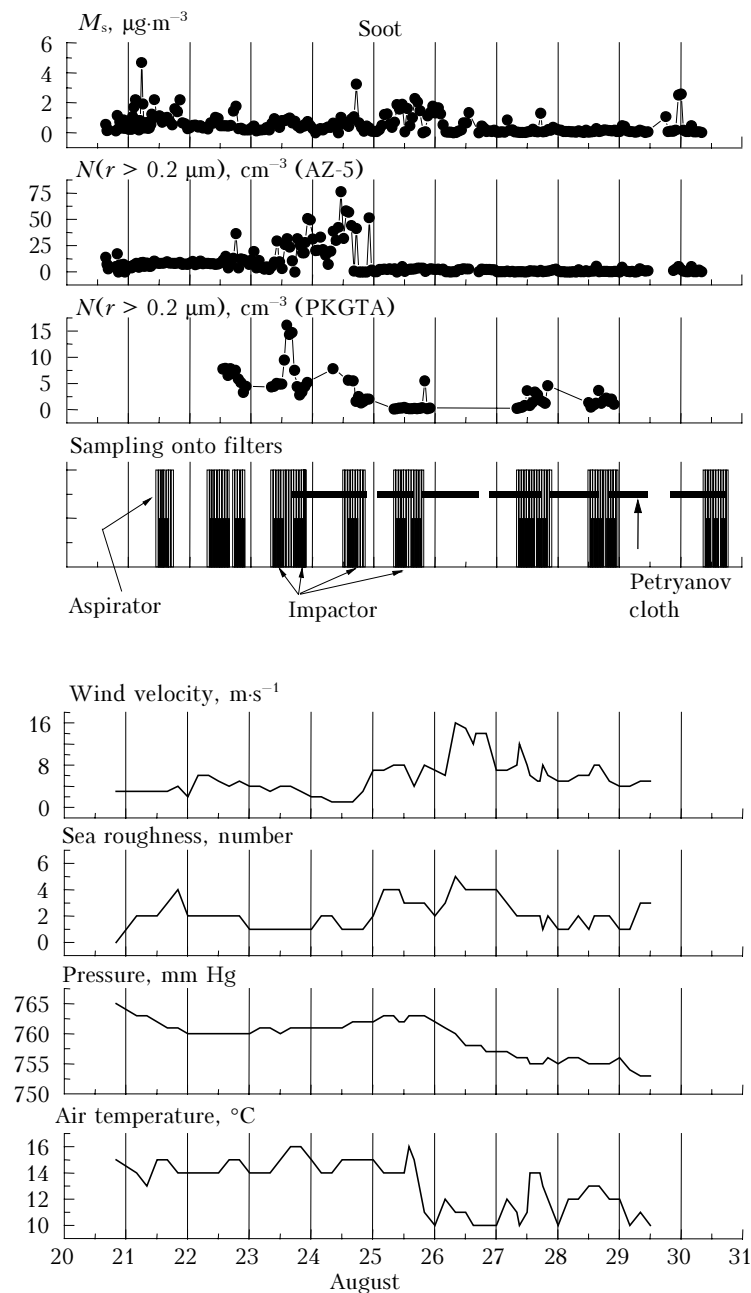


Fig. 3. General time behavior of the measured parameters.

Disperse composition of aerosol

Figure 4 depicts the averaged (over the time intervals of aerosol sampling onto the filters) volume size distributions for the data obtained with a PKGTA and an automated AZ-5 counter. One can see a good agreement between the data of different counters. The particle size distribution function is characterized by the absence of a pronounced peak in the submicron part, which we and other investigators noticed in other regions of the Global Ocean.⁶

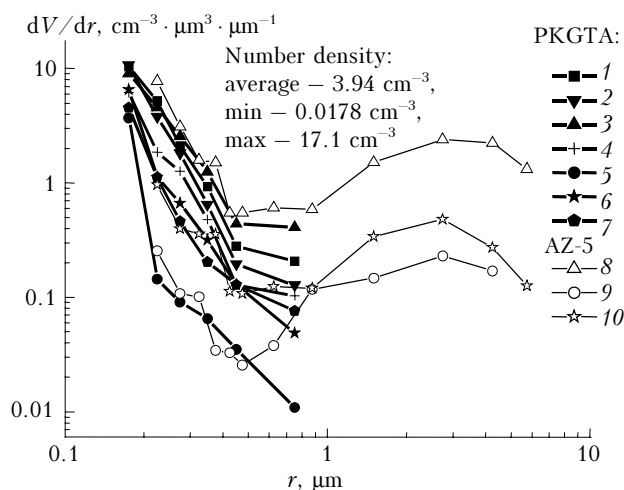


Fig. 4. Volume size distributions according to data obtained with a PKGTA and an AZ-5 counter. Data are averaged over the intervals of aerosol sampling onto the filters. PKGTA: August 22 (1), 22 (2), 23 (3), 24 (4), 25 (5), 27 (6), and 28 (7); AZ-5: August 23 (8), 25 (9), and 27 (10).

The concentration of submicron particles increases as approaching the continent and industrial regions. The coarse fraction becomes more pronounced with the increase of the wind velocity (see Fig. 3).

The average number density of aerosol particles was 3.94, while the minimum and the maximum ones amounted to 0.0178 and 17.1, in cm^{-3} , which is characteristic of the regions with low aerosol content such as, for example, northern Atlantic and the Arctic.^{1,2,12}

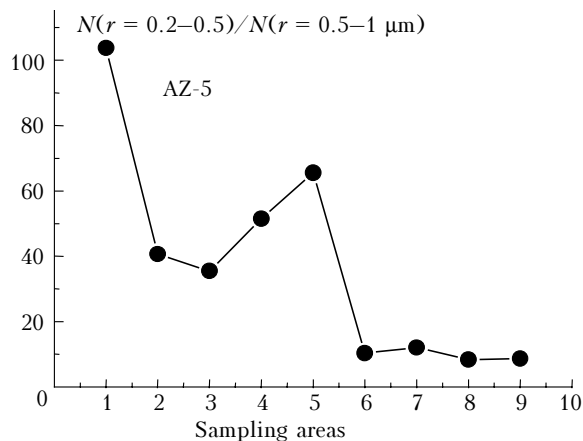


Fig. 5. Concentration ratio of submicron and coarse fractions.

The behavior of the particle size distribution function can be roughly described by the concentration ratio of the submicron and coarse particles N_{sub}/N_c . In our case, this integral parameter takes the form $N(r = 0.2–0.5)/N(r = 0.5–1 \mu\text{m})$, which allows us to estimate the behavior of the aerosol particle size distribution function in the range determining the optical characteristics of aerosol in the visible spectral region. The behavior of this integral parameter (Fig. 5) indicates that in the first five areas studied the size distribution is characterized by a relatively higher content of fine particles as compared to that in the areas 6–9, where the coarse fraction is more pronounced.

Some results on soot

The time behavior of the diurnally mean mass concentration of soot M_s (1) and the particle number density N obtained on the data collected with the AZ-5 counter (2) during the 55th mission of the *Professor Shtokman* RV is shown in Fig. 6.

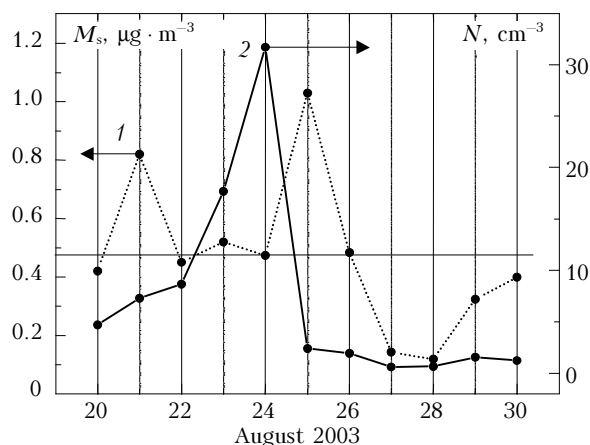


Fig. 6. Time behavior of the diurnally mean mass concentration of soot.

For the period of measurements, the diurnally mean values of the soot concentration in the surface atmosphere varied quite widely: on the average, from 0.1 to $1 \mu\text{g}/\text{m}^3$. Actually, the geography of the 55th mission of the *Professor Shtokman* RV covers the regions, which likely are under the impact of local anthropogenic sources of air pollution. Thus, the data on August 27 and 28 correspond to the northwestern measurement zone, most remote (roughly by 300 km) from the industrial region in the mouth of Severnaya Dvina River and are characterized by the lowest soot and aerosol contents (conditionally background region). The northern part of the route was also characterized by a relatively low level of the aerosol and soot content (August 22). The increased levels of the aerosol load were observed in the route parts adjacent to the mouth of Severnaya Dvina River (August 24) and in the southern part of the mission route (August 25).

The possible cause for the discrepancy between the maximum diurnal values of the aerosol particle number density and the soot concentration may be unstable weather conditions on August 24 through

26, because of the change of air masses (cyclone–anticyclone), increased wind speed and sea roughness, and significant variations in the air pressure and temperature. Besides, precipitation contributed to the observed dynamics: fog was observed on August 24 until noon, and it rained during the entire day on August 26 and the evening of August 27. However, in spite of the noted discrepancies, the space and time tendencies in the aerosol number density and the soot concentration are, generally, close to each other.

The mass concentration of soot averaged over the corresponding intervals of aerosol sampling onto the filters is shown in Fig. 7.

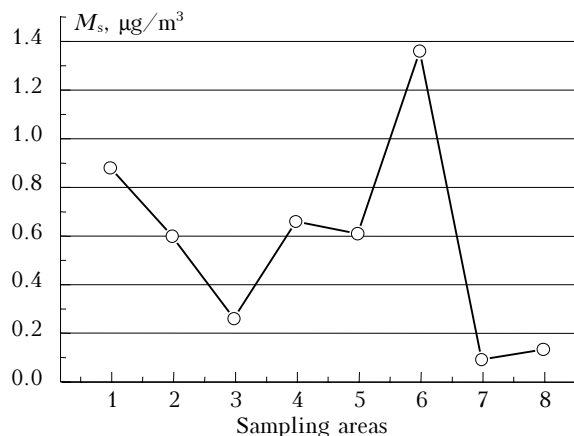


Fig. 7. Average values of the mass concentration of soot over the intervals corresponding to aerosol sampling onto the filters for chemical analysis.

Chemical analysis of the aerosol samples

Important sources of aerosol over the sea are salt particles produced due to seawater spraying and the collapse of air bubbles reaching the sea surface.¹³ These are the mechanisms that mostly determine disperse and chemical composition of the aerosol. To estimate the contribution of this source, it is important to analyze the concentration ratios of some chemical elements characteristic of seawater.

Consider the behavior of some ions, whose concentration is normalized to the concentration of Cl, which is the highest both in the seawater and in our samples.

In addition, calculate the "excess" of the ion content in the aerosol as compared to seawater as:

$$\Delta R_i = (R_i - kN_{\text{Cl}})/(kN_{\text{Cl}}),$$

where R_i is the concentration of the i th ion in aerosol; N_{Cl} is the concentration of Cl ions in aerosol; k is the ratio of R_i and N_{Cl} in seawater.

To analyze the contributions of the continental and marine sources to the ion composition of aerosol, we use the factor V_{cont} , which is the fill factor minus specific volume of the aerosol formed from seawater calculated by the following equation:

$$V_{\text{cont}} = \Sigma_i(R_i - kN_{\text{Cl}})/\Sigma_i R_i,$$

where $\Sigma_i R_i$ is the total concentration of all the ions measured in aerosol, and $\Sigma_i(R_i - kN_{\text{Cl}})$ is the total concentration of all the ions minus the ions formed from the sea water, and the fill factor of aerosol formed from the sea water is calculated as

$$V_{\text{ocean}} = 1 - V_{\text{cont}}.$$

The data on V_{cont} and V_{ocean} for the aspirator are shown in Fig. 8, from which it can be seen that in the first five areas studied the ion composition was formed by the continental sources and sea salts in roughly equal parts. In the following four areas, the ion composition was mostly formed by the marine sources.

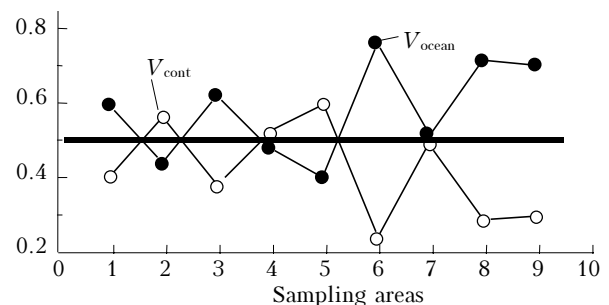


Fig. 8. Calculated V_{cont} and V_{ocean} , in fractions of unity.

The Cl^-/Na^+ ratio in our measurements (Fig. 9) is close to the value characteristic of seawater¹³ and falls within the ranges obtained by other authors^{13–17} (shaded area).

Analyzing the data presented in Fig. 9, one can notice identical behavior of the excesses and the normalized values for the ions, in particular, of the SO_4^{2-} and Ca^{2+} ions. The pronounced excess over the seawater ratio takes place for H^+ , HCO_3^- , NO_3^- , SO_4^{2-} , NH_4^+ , Ca^{2+} , K^+ , and Mg^{2+} , what points towards their non-sea-salt origin.

It is commonly accepted that the sulfate (SO_4^{2-}) aerosols are mostly represented by fine submicron-size particles. Aerosols containing calcium (Ca^{2+}) are mostly represented by coarse particles with the size greater than $1 \mu\text{m}$. Taking this into account, we have considered the concentrations of some ions normalized to the sulfate and calcium concentration (Fig. 10).

By analyzing and comparing the behavior of the following parameters: (a) the parameter $N(r = 0.2 - 0.5)/N(r = 0.5 - 1 \mu\text{m})$ (see Fig. 5); (b) the fill factors V_{cont} and V_{ocean} (see Fig. 8); and (c) the concentration ratios of some ions normalized to the concentrations of Cl^- , SO_4^{2-} , Ca^{2+} (Figs. 9 and 10), we can draw the following *qualitative conclusions from the data obtained in the experiment with the aspirator*:

- Cl^- and Na^+ ions are largely present in coarse particles and have the sea-salt origin;
- Ca^{2+} ions are also largely present in coarse particles, but have the continental origin;
- SO_4^{2-} and NH_4^+ ions are mostly contained in the fine aerosol and have the continental origin;
- HCO_3^- ions can be present in both fine and coarse particles and have both the sea-salt and continental origin;

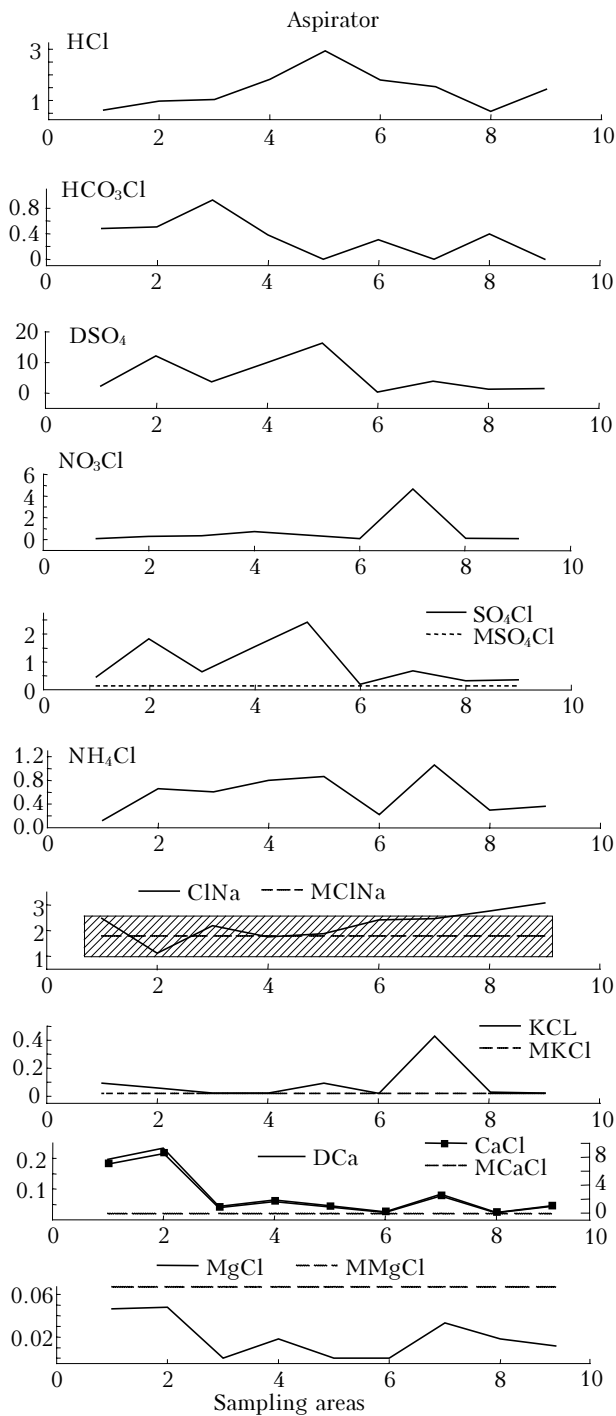


Fig. 9. Concentrations of some ions normalized to the Cl concentration and excess. Designations: DSO₄ and DCa are the values of the corresponding excess calculated for the SO₄²⁻ and Ca²⁺ ions; HCO₃Cl, NO₃Cl, SO₄Cl, NH₄Cl, KCl, CaCl, and MgCl are the concentration ratios of the HCO₃⁻, NO₃⁻, and other ions to Cl⁻; MClNa, MKCl, MClCa, MClSO₄, ... are the concentration ratios of Cl⁻, K⁺, and other ions to Na⁺ or Cl⁻ of the seawater.

– the maximum concentrations of the NO₃⁻ and K⁺ ions are observed in the Gulf of Kandalaksha; the sea and the continent contribute roughly equally to the formation of the concentrations of these ions;

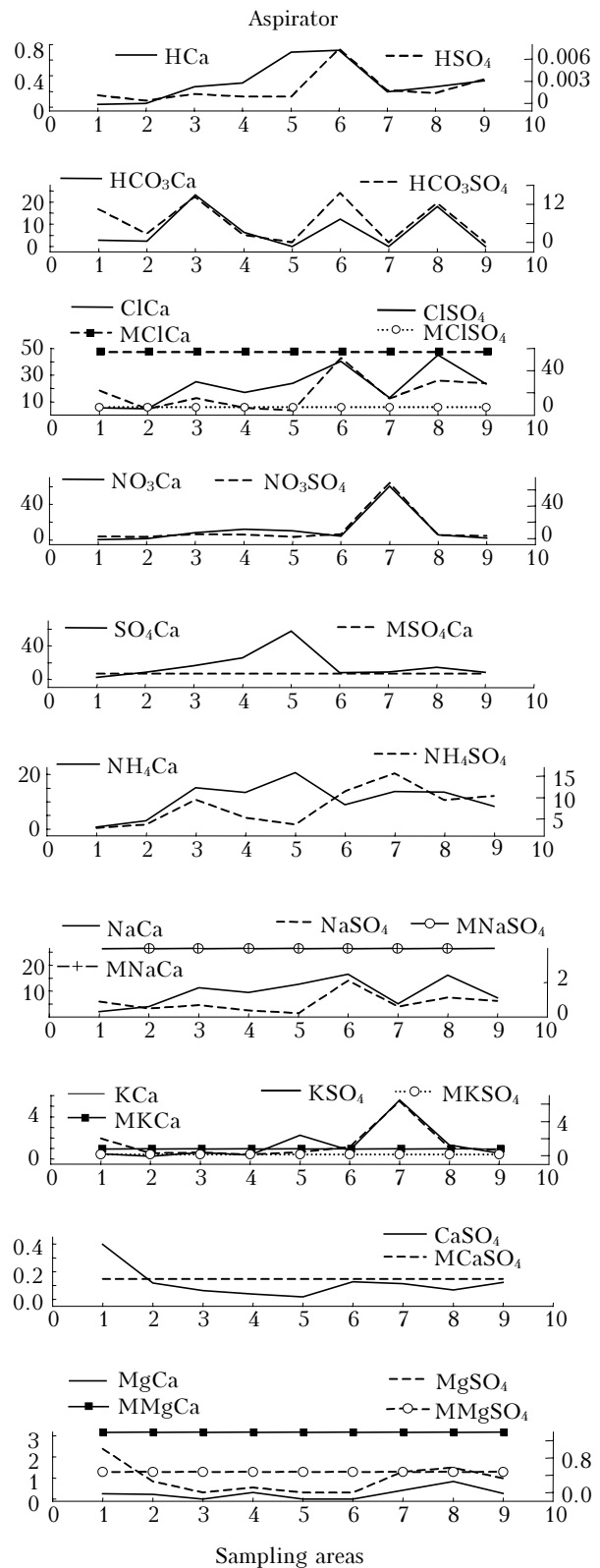


Fig. 10. Concentrations of some ions normalized to the concentration of SO₄²⁻ and Ca²⁺. Designations: HCa, HCO₃Ca, ... are the concentration ratios of H⁺, HCO₃⁻, ... ions to Ca²⁺; HSO₄, HCO₃SO₄, ... are the concentration ratios of H⁺, HCO₃⁻, ... ions to SO₄²⁻; MClCa, MClSO₄, ... are the concentration ratios of Cl⁻ and Ca²⁺, Cl⁻ and SO₄²⁻, ... for seawater.

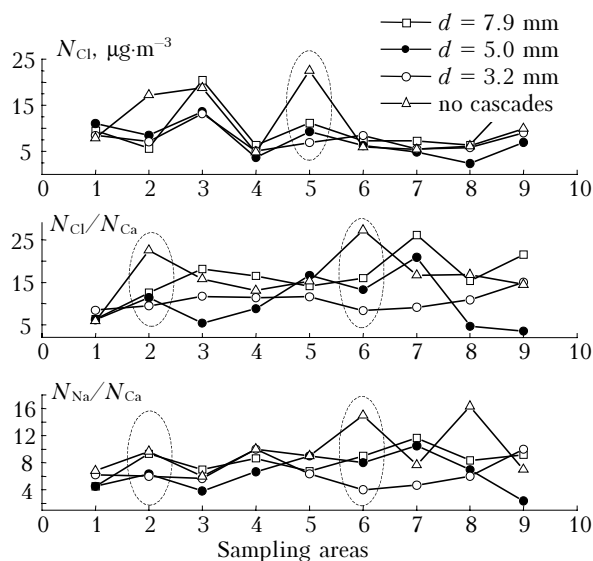


Fig. 11. Concentration of Cl^- , and Cl^- and Na^+ normalized to Ca^{2+} according to data obtained with and without the impactor cascades.

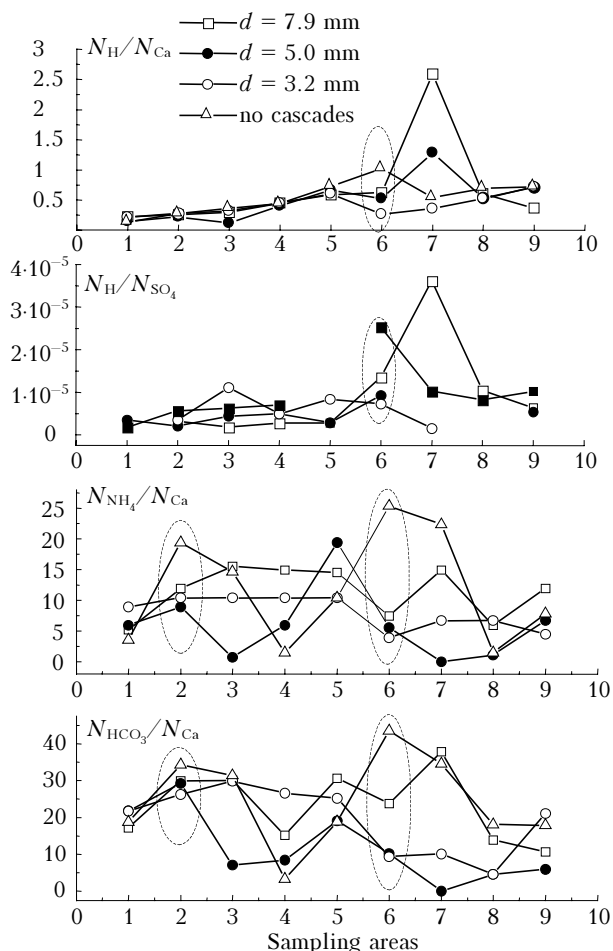


Fig. 12. Concentrations of some ions normalized to the concentrations of SO_4^{2-} and Ca^{2+} for the data obtained with and without impactor cascades.

– the increased concentrations of Mg^{2+} ions are observed in the regions close to the continental industrial sources of aerosol, and the concentration

ratio of this ion to other ions is much lower than for seawaters.

Figures 11 and 12 illustrate the separation of the contributions from every impactor cascade for the Cl^- ions in the 5th sampling area, $\text{H}^+/\text{Ca}^{2+}$ (normalized to Ca^{2+}), and $\text{H}^+/\text{SO}_4^{2-}$ in the 6th area, as well as $\text{Na}^+/\text{Ca}^{2+}$, $\text{NH}_4^+/\text{Ca}^{2+}$, $\text{HCO}_3^-/\text{Ca}^{2+}$, $\text{Cl}^-/\text{Ca}^{2+}$ in the 2nd and 6th areas (these areas are outlined by the dashed curve).

In other cases, this separation does not occur. This may be explained by several reasons: first, the statistically insufficient material; second, the aerosol inhomogeneity along the sampling route, third, the presence of ions only in fine particles, which are not separated by the impactor; and, fourth, the errors of the measurement technique.

Despite the variety of interferences, the results obtained confirm the earlier conclusions on the aspirator and illustrate the capabilities of the impactor method.

Conclusions

The data have been obtained over the sea surface on the correlation between individual chemical elements (ions) of the aerosol matter and the size of aerosol particles.

The data on the ion composition of the aerosol matter collected with the impactor allows one to judge on the relation between the microphysical parameters and the ion composition for the aspirator data and refining the ion composition of coarse aerosol particles (greater than $1\ \mu\text{m}$).

Acknowledgments

The authors are grateful to the crew of the *Professor Shtokman* research vessel for the help during the research mission and to Vas.V. Pol'kin for participation in the measurements.

This work was supported, in part, by the Presidium of the Russian Academy of Sciences (Project 14.1 "Global Ocean"), the RAS Division of Earth Sciences (Project "Nanoparticles in Earth's External and Internal Spheres"), and the Ministry of Industry, Science and Technologies of Russia (grant No. NSh-1940.2003.5).

References

1. V.P. Shevchenko, A.P. Lisitsyn, A.A. Vinogradova, V.V. Smirnov, V.V. Serova, and R. Stein, *Atmos. Oceanic Opt.* **13**, Nos. 6–7, 510–532 (2000).
2. V.P. Shevchenko, *Berichte zur Polar- und Meeresforschung*, No. 464, 149 (2003).
3. V.V. Pol'kin, L.P. Golobokova, V.S. Kozlov, V.B. Korobov, A.P. Lisitsyn, M.V. Panchenko, M.A. Peskova, V.P. Shevchenko, and T.V. Khodzher, in: *Abstracts of Papers at X Workshop on Siberian Aerosols*, Tomsk (2003), p. 17.
4. V.V. Pol'kin, Vas.V. Pol'kin, M.V. Panchenko, V.S. Kozlov, A.P. Lisitsyn, and V.P. Shevchenko, in: *XV International Scientific School on Marine Geology "Geology of Seas and Oceans"* (GEOS, Moscow, 2003), Vol. 2, pp. 112–113.

5. M.V. Panchenko, V.V. Pol'kin, L.P. Golobokova, M.P. Chubarov, O.G. Netsvetaeva, and V.M. Domysheva, *Atmos. Oceanic Opt.* **10**, No. 7, 460–466 (1997).
6. S.M. Sakerin, D.M. Kabanov, and V.V. Pol'kin, *Atmos. Oceanic Opt.* **8**, No. 12, 981–988 (1995).
7. V.S. Kozlov, M.V. Panchenko, A.G. Tumakov, V.P. Shmargunov, and E.P. Yausheva, *J. Aerosol Science* **28**, Suppl. 1, S231–S232 (1997).
8. A.D.A. Hansen, H. Rosen, and T. Novakov, *Sci. Total Environ.* **36**, No. 1, 191–196 (1984).
9. H. Rosen and T. Novakov, *Appl. Opt.* **22**, No. 1, 1265–1267 (1983).
10. A.D. Clarke, *Appl. Opt.* **21**, No. 16, 3021–3031 (1982).
11. A.M. Baklanov, V.S. Kozlov, M.V. Panchenko, A.N. Anki-
lov, and A.L. Vlasenko, *J. Aerosol Sci.* **29**, 919–920 (1998).
12. D.M. Kabanov, M.V. Panchenko, V.V. Pol'kin, and S.M. Sakerin, in: *Abstracts of Papers at IV Symp. on Atmos. Ocean Optics*, Tomsk (1997), pp. 116–117.
13. R. Chester, *Marine Geochemistry* (Unwin Hyman, London, 1990), 698 pp.
14. L.S. Ivlev, *Chemical Composition and Structure of Atmospheric Aerosols* (Leningrad State University, Leningrad, 1982), 358 pp.
15. V.D. Korzh, *Dokl. Akad. Nauk SSSR* **292**, No. 4, 822–827 (1987).
16. V.S. Savenko, *Dokl. Akad. Nauk SSSR* **299**, No. 2, 465–468 (1988).
17. V.K. Donchenko and L.S. Ivlev, in: *Proc. of III Int. Conf. on Natural and Anthropogenic Aerosols* (St. Petersburg, 2001), pp. 41–52.